

Full Length Research Paper

Effect of milling conditions on the formation of ZnFe_2O_4 nanocrystalline

O. M. Lemine

Department of Physics, College of Sciences, Al imam Mohammad Bin Saud Islamic University (IMSIU), P. O. Box 90950
11623 Riyadh, Saudi Arabia.

Accepted 15 March, 2013

The effects of milling parameters on the formation of ZnFe_2O_4 nanocrystalline are studied. Powder mixtures of ZnO and Fe_2O_3 were milled in high energy vibrant ball milling for different balls to powders mass ratio and milling times. X-ray diffraction and scanning electron microscopy are used to characterize the powders. A crystalline size and lattice parameter are obtained from Scherrer formula and the Nelson–Riley function respectively. It was found that the balls to powder mass ratio plays a key role on the formation of ZnFe_2O_4 nanocrystalline more than other parameters (type of mill and rotation speed). A spinel phase appears from 6 h of milling duration with balls to powder ratio of 10:1 but nevertheless, the Fe_2O_3 and ZnO disappear if the milling time was further increased to 24 h. For balls to powders mass ratio of 20:1, the obtained zinc ferrite phase seems to be pure after 12 h milling. The effect of the different parameters is discussed in detail.

Key words: Zinc-Ferrite, nanocrystalline, ball milling, scanning electron microscope (SEM), X-ray diffraction.

INTRODUCTION

Zinc ferrite (ZnFe_2O_4) is of interest not only to basic research in magnetism, but also has great potential in technological application, such as magnetic materials, gas sensors, catalysts, photocatalysts and absorbent materials (Xu et al., 2011). The structure of the spinel oxides AB_2O_4 consists of the close-packed face cubic centred (FCC) arrangement of oxygen atoms, with two non-equivalent crystallographic tetrahedral A and octahedral B sites. In zinc ferrite, the Zn^{2+} and Fe^{3+} ions can be distributed over the A and B sites, and therefore the formula is sometimes represented by $(\text{Zn}_{1-\delta}\text{Fe}_\delta)[\text{Zn}_\delta\text{Fe}_{2-\delta}]\text{O}_4$, where the part between the round brackets represent, are the atoms at the A sites, the part between square brackets are the atoms at the B sites and δ is a measure of the fraction of Fe^{3+} on the A sites and is called the inversion parameter. δ is 1 for a

perfectly inverse spinel, $2/3$ for the random arrangement and 0 for a perfectly normal spinel. Several methods have been used for the preparation of ZnFe_2O_4 nanocrystalline such as co-precipitation, aerogel and hydrothermal method (Jiang et al., 1999; Shenoy et al., 2004; Yu et al., 2003). Among all this techniques mechanical alloying (MA) turns to be the mostly used to prepare nanocrystalline due to its simplicity, low cost and its ability to produce large volumes. Mechanical alloying influences phase ratio, particle morphology, particle size distribution, and microstructure of the final product. Milling parameters of importance include type of mill, milling container, speed, time, grinding medium, ball-to-powder weight ratio, milling atmosphere, process control agent and milling temperature. However, the most important parameters are the milling time, speed and

ball-to-powder ratio (Suryanarayana, 2000). Several groups have been interested by the production of ZnFe_2O_4 nanocrystalline by mechanical alloying using a start materials ZnO and $\alpha\text{-Fe}_2\text{O}_3$ powders (ZHAO et al., 2010; Verdier et al., 2005; Jean and Nachbaur, 2008; Nachbaur et al., 2009). For example Nachbaur et al. (2009) and Verdier et al. (2005) studied the effect of milling times with a fixed balls to powders mass ratio (20:1) and speed rotation. Jean and Nachbaur (2008) were interested by the influence of disc and vials velocity on the end products. ZHAO et al. (2010) obtained zinc ferrite after 40 h milling with balls to powder ratio of 20:1.

A common point between all the works that most of them used high energy planetary milling to prepare the sample. The aim of this work is to give an additional contribution to understand the influence of the type of mill (vibrant mill), the balls to powders mass ratio and the milling times on the formation of ZnFe_2O_4 nanocrystalline.

EXPERIMENTAL

Commercially powders of hematite ($\alpha\text{-Fe}_2\text{O}_3$) and zinc oxide (ZnO) are used with equal molar (1:1) and were introduced into a stainless steel vials with stainless steel balls (12 and 6 mm in diameter) in a high energy mill (SPEX 8000 mixer mill). Different milling times were considered (6, 12 and 24) and two values of the balls to powders mass ratio were used (10:1 and 20:1). X-ray powder diffraction (XRD) measurements were performed using Shimadzu diffractometer (θ - 2θ) equipped with Cu-K α radiation ($\lambda=1.5418$ Å). The crystallite size was calculated from the Scherer formula:

$$D = \frac{K\lambda}{B \cos \theta} \quad (1)$$

where $\lambda=1.5418$ Å, K is a constant whose value is approximately 0.9 and B (rad) is the width of peak. B (in rad) was determined as full width at half-maximum (FWHM). Particles morphology of our samples was investigated using Nova 200 NanoLab field emission scanning electron microscope (FE-SEM).

RESULTS AND DISCUSSION

Figure 1 shows the XRD patterns for Zinc oxides, hematite and the initial hematite and zinc oxide mixture, before ball milling. The patterns of un-milled ZnO, $\alpha\text{-Fe}_2\text{O}_3$ and (ZnO + $\alpha\text{-Fe}_2\text{O}_3$) mixture powders show a series of strong and narrow peaks characteristic for high quality ZnO and $\alpha\text{-Fe}_2\text{O}_3$ crystals. The crystallite size for the started powders ZnO and $\alpha\text{-Fe}_2\text{O}_3$ are 150-300 nm and 200-300 nm, respectively.

Figure 2 shows the XRD patterns for the sample milled for different times (6-24 h) and balls to powder ratio of 10:1. XRD pattern of the un-milled mixture is added to see the line positions of the initial oxides. Table 1 shows the phases obtained with different milling parameters. With increasing the milling time, the diffraction peaks became broader and their relative intensity decreases, as shown in Figure 2b-d. This effect is a typical behaviour of

materials after milling and attributed usually the presence of crystallite with small size and internal strain induced by mechanical deformation. Similar results were obtained for milling of ZnO and $\alpha\text{-Fe}_2\text{O}_3$ powders separately (Lemine, 2009). Regarding the decrease of the relative intensity of the peaks, it can be seen that the decrease of the ZnO peaks was more obvious, compared with that of $\alpha\text{-Fe}_2\text{O}_3$ for longer milling times. That can be explained by the amorphization of ZnO or may be by the diffusion of ZnO into $\alpha\text{-Fe}_2\text{O}_3$. But the second reason seemed more reasonable due to all milling times, the ZnO peaks remained. In addition, the equal molar (1:1) of ZnO and $\alpha\text{-Fe}_2\text{O}_3$ used in the preparation of the samples explained that ZnO diffused into Fe_2O_3 crystal lattice during mechanical alloying process.

After 6 h milling, it can be seen that the zinc ferrite phase, ZnFe_2O_4 appears and coexists with the remaining hematite and Zinc oxides phases. The presence of zinc ferrite is revealed by the lines around 17.5° (spinel phase) and can be explained by the solid state reaction of ZnO and $\alpha\text{-Fe}_2\text{O}_3$. The same result was obtained for longer milling times (12 and 24 h) and $\alpha\text{-Fe}_2\text{O}_3$ and ZnO are still present. For the same milling times, several research groups obtained a pure zinc ferrite (ZHAO et al., 2010; Verdier et al., 2005; Jean and Nachbaur, 2008; Nachbaur et al., 2009). For example Nachbaur et al. (2009) observed that after 12 h of milling, the main phase is zinc ferrite. After 24 of milling the phase obtained is a pure zinc ferrite. Recently ZHAO et al. (2010) obtained zinc ferrite phase after 30 h. The difference with the current results can be explained by the value of balls to powders mass ratio used by all the groups (20:1, in this study 10:1 was used). Nevertheless, the Fe_2O_3 and ZnO disappear if the milling time was further increased to 24 h. We can conclude that the balls to powder mass ratio plays a key role of the formation of ZnFe_2O_4 nanocrystalline more than other parameters (type of mill and rotation speed).

In order to compare the effect of the type of mill, we have prepared one sample with the same ball to powders mass ratio used by the other groups (20:1). Considering that the rotation speed of high energy vibrant mill (SPEX 8000D) is higher than that used for planetary milling (500 rpm), we used only one milling time of 12 h and the XRD patterns are shown in Figure 3. It is clear from the figure that (h k l) values of each peak corresponding to the zinc ferrite. XRD pattern of the sample exhibits the formation of single-phase cubic spinel structure. The characteristic peaks for the spinel Zn-ferrite appear as the main crystalline phases. The average crystallite size (10 nm) was estimated from the most intense peak, corresponding to (311) reflection by using the Debye-Scherrer formula. The interplanar spacing, d_{hkl} (h, k, l are Milles indices), were calculated from the Bragg equation (Cullity, 1979).

$$2d_{hkl} \sin \theta = n\lambda \quad (2)$$

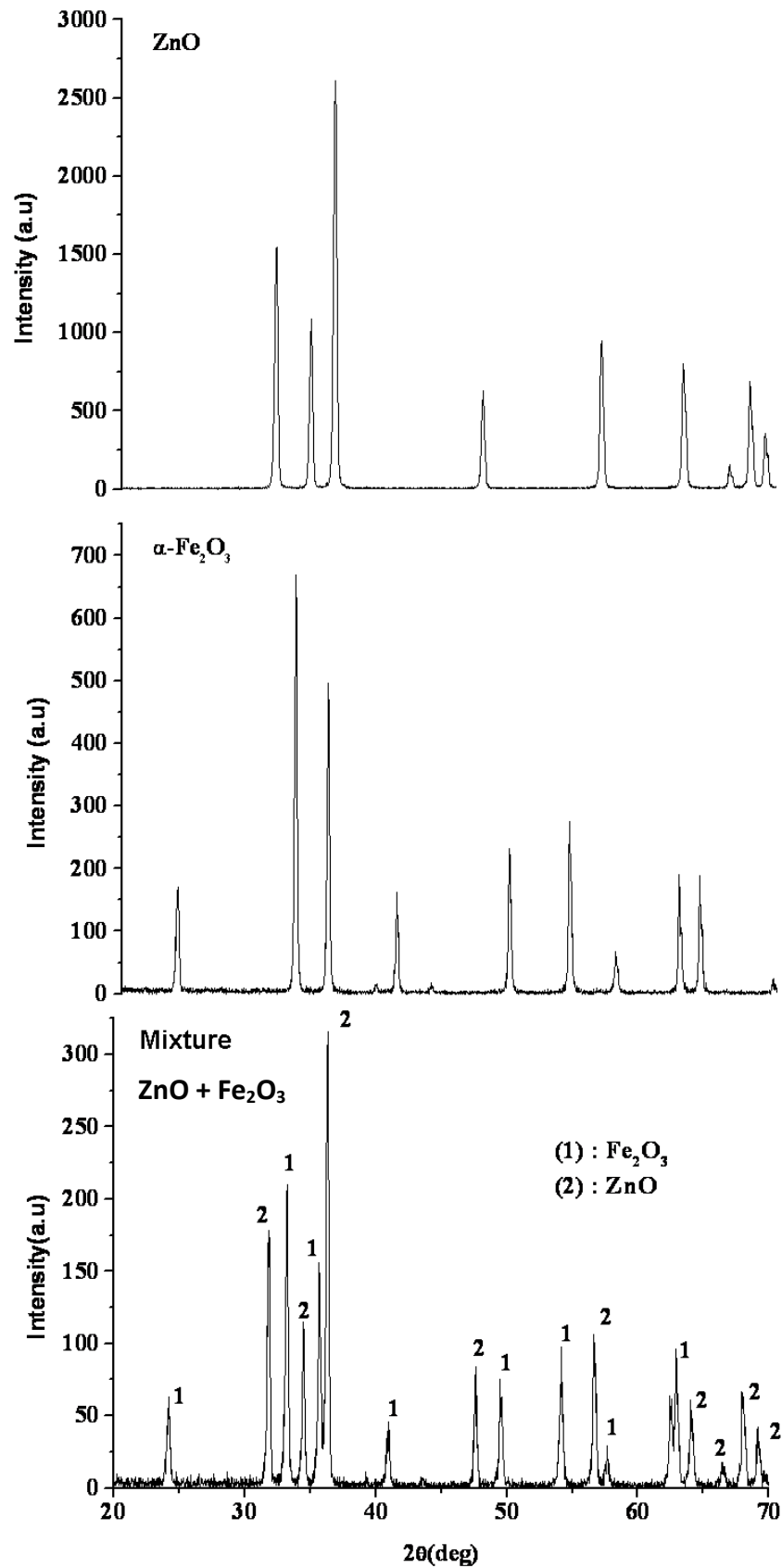


Figure 1. XRD patterns of ZnO, α - Fe_2O_3 and ZnO- α - Fe_2O_3 mixture.

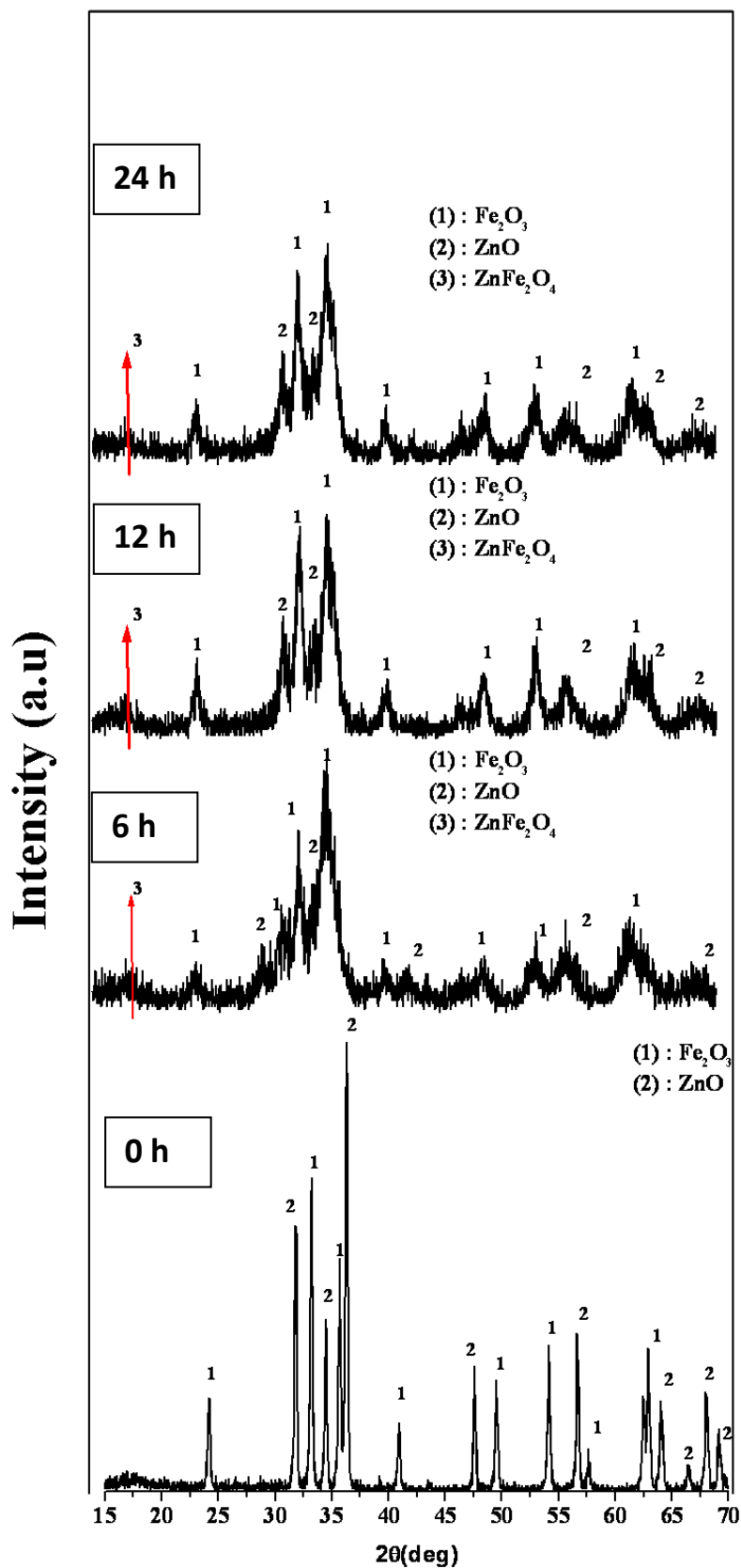
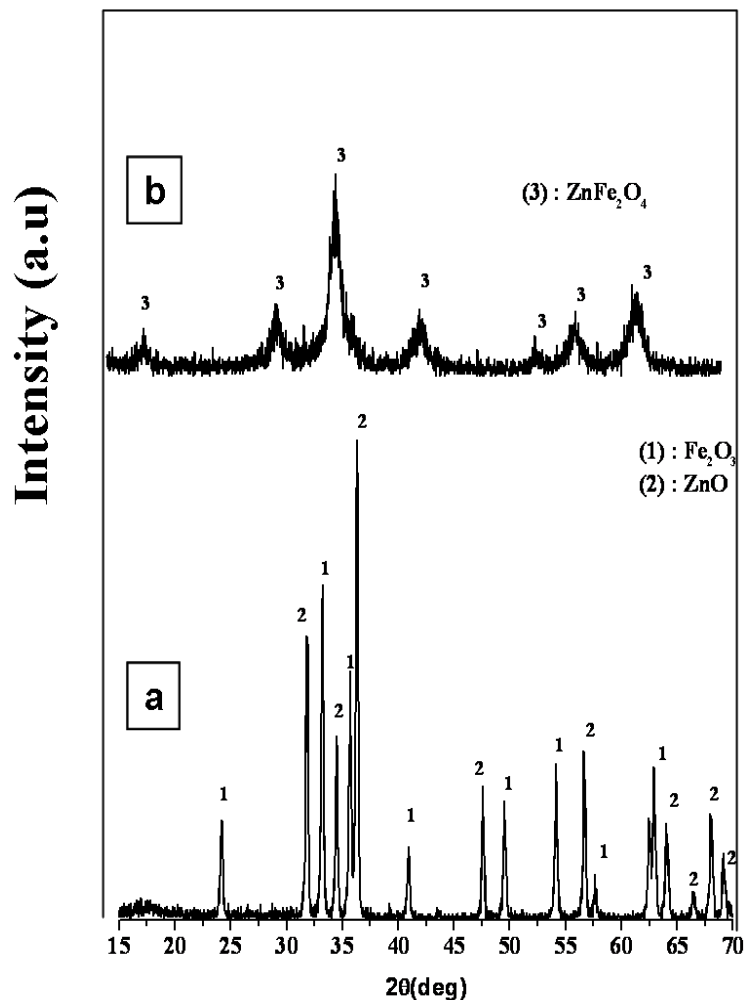


Figure 2. X-ray diffraction patterns of ball-milled ZnO–Fe₂O₃ mixture. For different milling times and balls to powder mass ratio of 10:1.

Table 1. The phase obtained with different milling parameters.

Variable	Milling times (h)	Phase
Balls to powders mass ratio 10:1	6	ZnFe ₂ O ₄ , ZnO and Fe ₂ O ₃
	12	ZnFe ₂ O ₄ , ZnO and Fe ₂ O ₃
	24	ZnFe ₂ O ₄ , ZnO and Fe ₂ O ₃
Balls to powders mass ratio 20:1	12	ZnFe ₂ O ₄

**Figure 3.** X-ray diffraction patterns of ball-milled ZnO–Fe₂O₃ with balls to powder mass ratio of 20:1 : (a) before milling and (b) 12 h.

The lattice parameter, a , was determined by the relationship:

$$a = d_{hkl}(h^2 + k^2 + l^2)^{1/2} \quad (3)$$

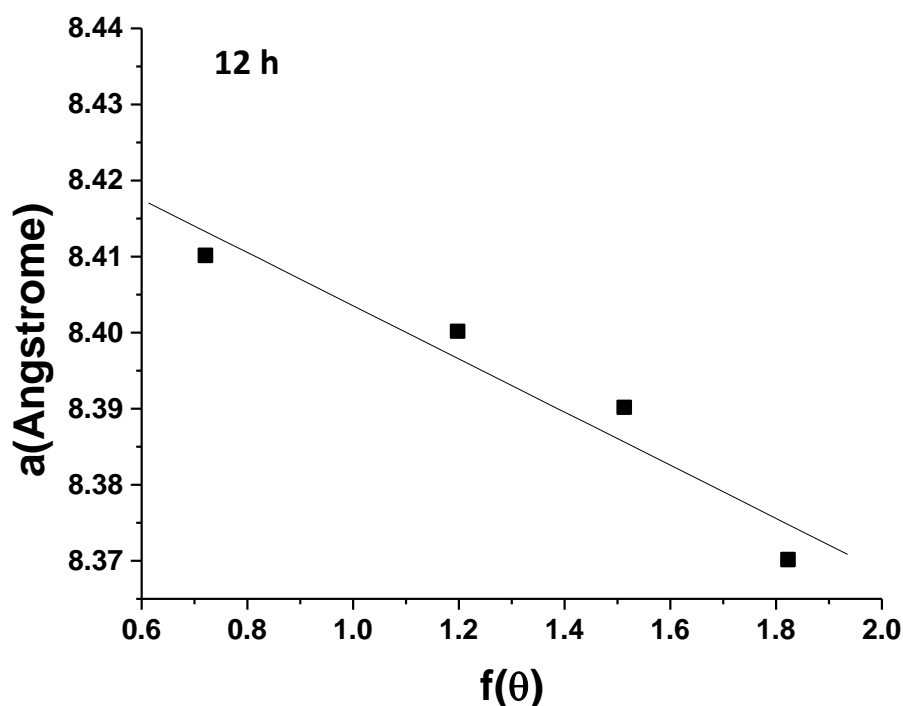
The values of the inter-planar spacing and zinc-ferrite lattice are reported in Table 2. The corrected values of

lattice parameter are estimated from the Nelson–Riley extrapolation method (Cullity, 1979). The values of the lattice parameter obtained from each reflected plane are plotted against the Nelson–Riley function $f(\theta)$:

$$f(\theta) = \frac{1}{2} \left(\frac{\cos^2 \theta}{\theta} + \frac{\cos^2 \theta}{\sin \theta} \right) \quad (4)$$

Table 2. Structural characteristics parameters.

Variable	Sample milled for 12 h			
(hkl)	2 θ (deg)	d_{hkl} (Å)	a_{hkl} (Å)	a (Å): Nelson-Riley function
(111)	18.26	4.85	8.400	
(220)	30.12	3	8.485	
(311)	35.46	2.53	8.391	
(400)	43.02	2.1	8.400	8.418
(422)	53.36	1.71	8.377	
(511)	57	1.61	8.365	
(440)	62.06	1.5	8.485	

**Figure 4.** Nelson-Riley plots for accurate measurement lattice constants of sample with balls to powder ratio 20:1 and milled for 12 h.

Where Θ is Bragg's angle and as straight line is obtained. The value of the lattice parameter was estimated from the extrapolation of the straight line to $f(\Theta) = 0$ (Figure 4). The obtained value was $a = 8.418 \text{ \AA}$ and it is slightly smaller than the 8.441 \AA value reported in Joint Committee on Powder Diffraction Standards (JCPDS) file (JCPDS 22-1012) but in agreement with value of $a = 8.437 \text{ \AA}$ reported recently by Nachbaur et al. (2009). Other groups obtained a values slightly larger than the value reported for bulk zinc ferrite, $a = 8.445 \text{ \AA}$ (Hakim et al., 2011) and $a = 8.449 \text{ \AA}$ (Ehrhardt et al., 2002). The contraction of the lattice parameter observed in our case and in the works published by Nachbaur et al., (2009) and

(Verdier et al., 2005) can be explained by the interpretation proposed by O'Neill (1992). For the compounds obtained by ceramic route with inversion parameters λ lower than 0.2, the cell parameter decreases with λ according to the following equation: $a \text{ (nm)} = 0.84423 - 0.001247 \lambda$. Sepelak et al. (1997) reported that this inversion leads to a contraction of the crystal lattice from 8.4432 (ceramic sample) to 8.4136 \AA (same sample milled for 24 min) but in our case it is difficult to conclude about an inversion phenomenon from our XRD results or to have a value for the inversion parameter. But it is interesting to note that in contrast to the bulk compound, the nanocrystalline ZnFe_2O_4 system

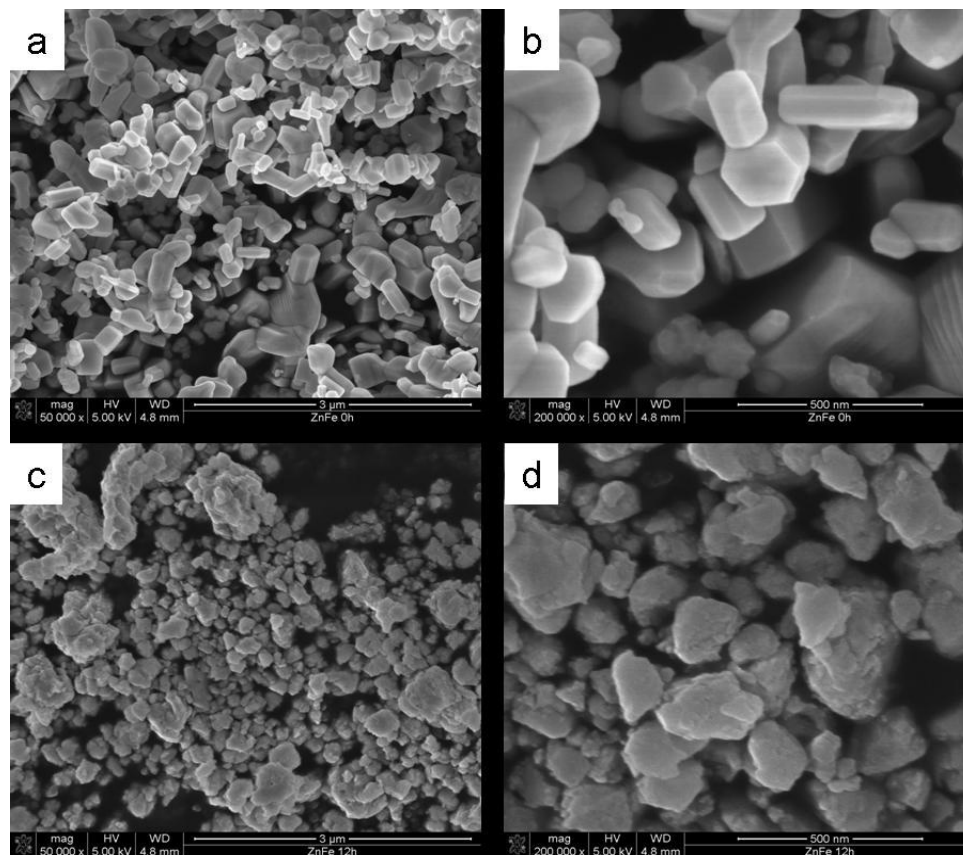


Figure 5. (a) SEM micrographs of mixtures (zinc oxides +hematite) powders as received (b) as received at high magnification (c) milled for 12h (c) milled for 12 h high magnification.

always shows up as a mixed spinel, of which the value of the inversion parameter λ is largely dependent on the synthesis procedure.

In general the process of synthesis of nanocrystalline zinc ferrite by ball milling of mixtures ($\text{ZnO}-\alpha\text{-Fe}_2\text{O}_3$) could be described as:



The difference in the results (milling times producing zinc ferrite or crystallites size) from one study to other depend on the type of milling used and the milling parameters such as balls to powder ratio, milling times and molar ratio between ZnO and Fe_2O_3 . Our results are similar with those obtained by Nachbaur et al. (2009) but they used planetary milling type with rotation speed of 500 rpm (in our case the vibrant milling with rotation speed of 1200 rpm) and that can explained the difference of milling times values.

SEM micrographs of the samples before and after milling are shown in Figure 5. It is clear that unmilled powder shows a different chap of powders due to zinc oxides and hematite powders (Figure 5a and b). After milling, a reduction of the crystallite size can be observed

(Figure 5c). High magnification images (Figure 5d) reveal clearly that large particles are in fact agglomerates of much smaller particles.

Conclusion

The synthesis process of ZnFe_2O_4 nanocrystalline by high energy ball milling the mixture of ZnO and Fe_2O_3 is affected by the milling parameters such as balls to powder mass ratio and milling time. It was found that the balls to powder mass ratio plays a key role of the formation of ZnFe_2O_4 nanocrystalline more than other parameters (type of mill and rotation speed). For balls to powder ratio of 10:1 and from 6 h milling, ZnFe_2O_4 appears and coexists with the remaining hematite and Zinc oxides phases. For balls to powder ratio of 20:1 the spinel Zn-ferrite appear as the main crystalline phases after 12 h of milling duration.

REFERENCES

Cullity BD (1979). Elements of X-ray Diffraction, Addison-Wesley, Reading, Massachusetts P. 356.

- Ehrhardt H, Campbell SJ, Hofmann M (2002). Structural evolution of ball-milled ZnFe_2O_4 . *J. Alloys Compd.* 339(2002):255-260.
- Hakim MA, Haque M, Huq M, Nordblad P (2011). Spin-glass-like ordering in the spinel ZnFe_2O_4 ferrite. *406(1)*:48-51.
- Jean M, Nachbaur V (2008). Determination of milling parameters to obtain mechanosynthesized ZnFe_2O_4 . *J. Alloys Compd.* 454(1-2):432-436.
- Jiang JZ, Wynn P, Morup S, Okada T, Berry FJ (1999). Magnetic structure evolution in mechanically milled nanostructured ZnFe_2O_4 particles. *Nanostruct. Mater.* 12:737-740.
- Lemine OM (2009). Microstructural characterisation of nanoparticles using, XRD line profiles analysis, FE-SEM and FT-IR. *Superlattices Microst.* 45:576-582.
- Nachbaur V, Tauvel G, Verdier T, Jean M (2009). Mecanosynthesis of partially inverted zinc ferrite. *473(1-2)*:303-307.
- O'Neill HSC (1992). Temperature dependence of the cation distribution in zinc ferrite (ZnFe_2O_4) from powder XRD structural refinements. *Eur. J. Miner.* 4:571.
- Sepelak V, Tkacova K, Boldyrev VV, Wibmann S, Becker KD (1997). Mechanically induced cation redistribution in ZnFe_2O_4 and its thermal stability *Physica B* 234-236 (1997) 617.
- Shenoy SD, Joy PA, Anantharaman MR (2004). Effect of mechanical milling on coprecipitated ultrafine zinc ferrites. *J. Magn. Magn. Mater.* 269:217-226.
- Suryanarayana C (2000). Mechanical alloying. *Progr. Mater. Sci.* 46:1-184.
- Verdier T, Nachbaur V, Jean M (2005). Mechano-synthesis of zinc ferrite in hardened steel vials: Influence of ZnO on the appearance of Fe(II). *J. Solid State Chem.* 178:3243-3250.
- Xu Y, Liang Y, Jiang L, Wu H, Zhao H, Xue D (2011). Preparation and Magnetic Properties of ZnFe_2O_4 Nanotubes, *J. Nanomaterials.* 2011.
- Yu SH, Fujino T, Yoshimura M (2003). Hydrothermal synthesis of ZnFe_2O_4 ultrafine particles with high magnetization, *J. Magn. Magn. Mater.* 256(2003):420-424.
- Zhao ZW, Ouyang K, Wang M (2010). Structural macrokinetics of synthesizing ZnFe_2O_4 by mechanical ball milling, *Trans. Nonferrous Met. Soc. China* 201131-1135.